

## **SURFACE MODIFICATION OF CaCO<sub>3</sub> NANOPARTICLES WITH SILANE COUPLING AGENT FOR IMPROVEMENT OF THE INTERFACIAL COMPATIBILITY WITH STYRENE-BUTADIENE RUBBER (SBR) LATEX**

ZHIYUAN YANG<sup>a</sup>, YANJUN TANG<sup>a, b, \*</sup>, JUNHUA ZHANG<sup>c</sup>

<sup>a</sup>*Key Laboratory of Advanced Textile Materials and Manufacturing Technology, Ministry of Education, Zhejiang Sci-Tech University, Hangzhou, 310018, China*

<sup>b</sup>*State Key Lab of Pulp and Paper Engineering, South China University of Technology, Guangzhou, 510640, China*

<sup>c</sup>*Engineering Research Center for Eco-Dyeing & Finishing of Textiles, Ministry of Education, Zhejiang Sci-Tech University, Hangzhou, 310018, China*

To improve the nano-particle dispersion and interfacial compatibility of CaCO<sub>3</sub> nanoparticles with styrene-butadiene rubber (SBR) latex, the surface of CaCO<sub>3</sub> nanoparticles was modified with silane coupling agent. The microstructure and surface behavior of modified CaCO<sub>3</sub> nanoparticles were systematically investigated by FTIR, TGA, XRD, TEM, contact angle measurement and rheological measurement. According to the spectra of FTIR, it can be inferred that silane coupling agent was successfully grafted onto the surface of CaCO<sub>3</sub> nanoparticles after modification. TGA further confirmed that the highest grafting ratio of silane coupling agent on the surface of CaCO<sub>3</sub> nanoparticles was about 1.5%. It was indicated by XRD that there was no marked change of the crystal form of CaCO<sub>3</sub> nanoparticles after surface modification. Contact angle measurement revealed that the surface hydrophobicity of CaCO<sub>3</sub> nanoparticles was remarkably enhanced with the increase of grafting ratio of silane coupling agent. TEM showed that modified CaCO<sub>3</sub> nanoparticles displayed good dispersibility and the average particle size was less than 100nm. In addition, rheological measurement was employed to evaluate the interfacial compatibility of CaCO<sub>3</sub> nanoparticles with SBR latex. The results demonstrated that the apparent viscosity of modified CaCO<sub>3</sub> nanoparticles/SBR composites were obviously lower than that of unmodified CaCO<sub>3</sub> nanoparticles/SBR composites.

(Received February 19, 2013; Accepted April 1, 2013)

*Keywords:* CaCO<sub>3</sub> nanoparticles; Silane coupling agent; Surface modification; Contact angle; Interfacial compatibility

### **1. Introduction**

In recent years, great attentions have been paid to nanoparticles due to its special features, such as surface effects, small size effects, boundary side effects and the macroscopic quantum effects [1-3]. However, the aggregation of nanoparticles owing to the overhigh surface energy and surface polarity weakens their special nature [4]. Nanoparticle surface properties, which can be altered by means of surface modification, play a very important role in both dispersion and interfacial compatibility of nanoparticles. The surface properties of nanoparticles after modification can be significantly improved, suggesting that surface modification is necessary sometimes before its application.

CaCO<sub>3</sub> nanoparticles, as a high-yield and cheap nano-material, have been widely used in some fields of rubber, plastics, building materials, coating, papermaking and so on [5-9], and the

---

\*Correspondence author: tangyj@zstu.edu.cn

surface modification of CaCO<sub>3</sub> nanoparticles can be achieved by inorganic or organic surface modifiers under given conditions. Wang [10] treated CaCO<sub>3</sub> nanoparticles with a self-made surface modifier (an amine salt of the acrylic acid ester) to enhance the properties of architectural coatings. A significant improvement in dirt resistance, scrub resistance, water resistance and aging resistance was obtained for coating containing modified CaCO<sub>3</sub> nanoparticles. Xue [11] grafted polyethyleneglycol phosphate (PGP) onto the surface of CaCO<sub>3</sub> nanoparticles designed for the in-situ preparation of poly ethylene terephthalate (PET). It was found that the synthetic composites with modified CaCO<sub>3</sub> exhibited a better dispersion of nanoparticles, a higher polymerization degree and a better thermal stability than that with unmodified CaCO<sub>3</sub> nanoparticles. Morel [12] used an alkyl- and a fluoro-alkoxysilane derivative to modify nanosized precipitated silica coated calcium carbonate fillers, and a significant hydrophilicity decrease was observed after modification. Tran [13] prepared one core-shell typed and surface-modified nanosized precipitated calcium carbonate with highly hydrophobic properties through the adsorption of sodium stearate in aqueous solution. In our previous work [14], palmitic acid was used to modify CaCO<sub>3</sub> nanoparticles and a comparative study on the crystal structure and thermal decomposition behavior between CaCO<sub>3</sub> nanoparticles, modified CaCO<sub>3</sub> nanoparticles, and CaCO<sub>3</sub> microparticles was made. According to FTIR, it was shown that a red shift (35 cm<sup>-1</sup>) of the infrared absorption peak (C-O) of modified and unmodified CaCO<sub>3</sub> nanoparticles was observed. TGA revealed that CaCO<sub>3</sub> nanoparticles, modified CaCO<sub>3</sub> nanoparticles and CaCO<sub>3</sub> microparticles decomposed at 735.0 °C, 764.7 °C and 775.6 °C, respectively. However, the effect of palmitic acid amount on the dispersion properties and interfacial compatibility of CaCO<sub>3</sub> nanoparticles was not investigated, and the possible surface modification mechanism as well as the potential application was not further studied.

In the present work, surface modification of CaCO<sub>3</sub> nanoparticles was achieved with silane coupling agent. The effect of the silane coupling agent on the microstructure and surface behavior of CaCO<sub>3</sub> nanoparticles was investigated. Based on the characterization and analysis, a possible surface modification mechanism was proposed. The nano-particle dispersion and interfacial compatibility of CaCO<sub>3</sub> nanoparticles as an additive in SBR latex were further investigated.

## **2. Experimental**

### **2.1 Materials**

A commercially available precipitated calcium carbonate with an average particle size of 50 nm was supplied by Asia Pulp & Paper Co., Ltd. Silane coupling agent, 3-methacryloxypropyltrimethoxysilane (KH570), with a purity of 98% was purchased as surface modifier from Nanjing Siliconesuper Chemical Co., Ltd. Anhydrous ethanol of analytical grade was obtained from Hangzhou Gaojing Fine Chemical Industry Co., Ltd. In addition, 0.1 mol/L of sulfuric acid solution was used to adjust pH value. Styrene-butadiene rubber (SBR) latex with a solid content of 45% was supplied by BASF. All chemicals above were used without further purification.

### **2.2 Surface modification of CaCO<sub>3</sub> nanoparticles**

The native CaCO<sub>3</sub> nanoparticles about 5 g were dispersed in 50 mL anhydrous ethanol with the aid of ultrasonication for 10 min. Silane coupling agent was hydrolyzed for 30 min at pH 4~5, and then CaCO<sub>3</sub> nanoparticles with a certain silane coupling agent were added into a 250 mL, three-necked, round-bottomed flask equipped with a mechanical stirrer and reacted at 70 °C for 2 h. Varied amounts of silane coupling agent (0 wt%, 1 wt%, 3 wt%, 5 wt% and 7 wt%) to CaCO<sub>3</sub> nanoparticles were employed. After the reaction, the products were filtrated and washed with anhydrous ethanol for at least 2 times to remove unreacted modifiers. Finally, the modified nanoparticles were dried in an oven at 65 °C for 24 h and cooled for 2 h at room temperature.

### **2.3 Preparation of CaCO<sub>3</sub>/SBR nano-composites**

CaCO<sub>3</sub>/SBR nano-composites were prepared by adding 1 wt% CaCO<sub>3</sub> nanoparticles

modified with varied amounts of silane coupling agent into SBR latex with a mechanical stirring of 800 rpm for 20 min.

## 2.4 Characterization methods

Before and after surface modification, the thermal behavior of various  $\text{CaCO}_3$  nanoparticle samples was determined by thermal gravimetric analysis (TGA) on thermal analyzer Pyris1 (Perkin Elmer, USA). The test was carried out in the air condition with the temperature increasing from room temperature to 750 °C at a heating rate of 10 °C/min.  $\text{CaCO}_3$  nanoparticle samples were prepared as KBr pellets and then the Fourier Transformed Infrared (FTIR) spectra was characterized on a Nicolet 5700 spectrometer (Thermo Fisher Scientific, USA) with a resolution of 0.09  $\text{cm}^{-1}$  at 400-4000  $\text{cm}^{-1}$ . X-ray diffraction (XRD) of  $\text{CaCO}_3$  nanoparticle samples was taken on a Diffractometer (X'TRA-055, ARL, Switzerland) with a  $\text{CuK}\alpha$  radiation ( $\lambda = 0.154$  nm) and the diffraction angle ranged from 20° to 50° at a scanning speed of 3°/min. The surface contact angle of  $\text{CaCO}_3$  nanoparticle samples, made as pellets with a thickness of 3 mm, was investigated using contact angle measuring instrument DSA10 (KRÜSS, Germany). The morphology analysis was carried out on transmission electron micrograph (TEM) analyzer (JEM-2100 Model, Japan) by placing several drops of diluted samples on copper sheets. To evaluate the interfacial compatibility of  $\text{CaCO}_3$  nanoparticles with SBR latex, rheological properties of  $\text{CaCO}_3$ /SBR nano-composites were measured by a commercially available Physica MCR301 advanced cylinder rotary rheometer (Anton Paar, Austria). The measurement was performed at 25 °C with a shear rate from 1  $\text{s}^{-1}$  to 500  $\text{s}^{-1}$ .

## 3. Results and discussion

### 3.1 FTIR spectra

Fig. 1 shows the FTIR spectra curves of  $\text{CaCO}_3$  nanoparticles treated with varied amounts of silane coupling agent. The assignments for the main FTIR bands of the modified  $\text{CaCO}_3$  nanoparticles are listed in Table 1. The broad absorption band between 3400  $\text{cm}^{-1}$  and 3200  $\text{cm}^{-1}$  are caused by the stretching vibration of absorbed water and the hydroxyl groups on the surface of nanoparticles. The bands at 2923  $\text{cm}^{-1}$  and 2852  $\text{cm}^{-1}$  can be assigned to the asymmetrical stretching vibration of methylene and the symmetrical stretching vibration of methyl groups, indicating that silane coupling agent has been successfully grafted onto the surface of  $\text{CaCO}_3$  nanoparticles after modification. This is in good agreement with the results reported by Sabzi [15]. But the peaks (at 2923  $\text{cm}^{-1}$  and 2852  $\text{cm}^{-1}$ ) are not very strong, which can be put down to the small amounts of modifiers. Peak at 1170  $\text{cm}^{-1}$  regarded as the characteristic absorption peak of  $-\text{OCH}_3$  did not occur, suggesting that the unreacted modifiers were removed by extraction in ethanol solution [20].

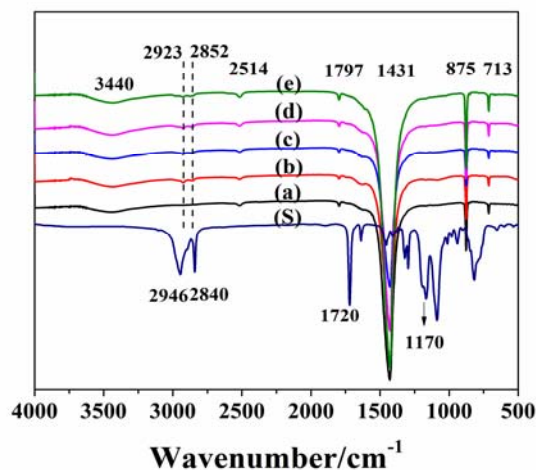


Fig. 1. FTIR spectra of  $\text{CaCO}_3$  nanoparticles modified with varied amounts of silane coupling agent (wt %): (a) 0, (b) 1, (c) 3, (d) 5, (e) 7 and (S) pure silane coupling agent.

Table 1. Characteristic peaks obtained from FTIR spectra of KH570-grafted CaCO<sub>3</sub> nanoparticles.

No.	Wavenumber(cm <sup>-1</sup> )	assignment
1	2946, 2923	C–H asymmetrical stretching mode (methylene group) [15-19]
2	2852, 2840	C–H symmetrical stretching mode (methylene group) [16,18-19]
3	2514	C–O asymmetric stretching mode + C–O symmetric stretching mode [17]
4	1797	C–O symmetric stretching mode + O–C–O bending (in-plane deformation) mode [17]
5	1720	C=O stretching mode [17]
6	1431	C–O asymmetric stretching mode [17]
7	1170	O–CH <sub>3</sub> stretching mode [20]
8	875	O–C–O bending (out-plane deformation) mode [17]
9	713	O–C–O bending (in-plane deformation) mode [17]

### 3.2 Thermal analysis

To figure out the amount of silane coupling agent grafted onto the surface of nanoparticles, thermo gravimetric analysis (TGA) technique was introduced. Fig. 2 illustrates the TGA curves of CaCO<sub>3</sub> nanoparticles before and after modification. A slight weight loss can be observed from 25 °C to 200 °C, which is due to the loss of physical adsorbed water on the surface. The weight loss between 200 °C and 670 °C is attributed to the removal of hydroxyl groups (–OH) on the surface of nanoparticles as well as the decomposition of grafted silane coupling agent. Above 670 °C, the weight loss drops sharply due to the release of CO<sub>2</sub> generated in the decomposition of CaCO<sub>3</sub>. The grafting ratio ( $\omega$ ) and the utilization efficiency ( $\alpha$ ) of silane coupling agent are expressed by the equations below:

$$\omega = \frac{m}{m + M_{CaCO_3}} \times 100\% \approx \frac{m}{M_{CaCO_3}} \times 100\% \quad (1)$$

$$\alpha = \frac{\omega}{\eta} \times 100\% \quad (2)$$

In equation (1), where  $M_{CaCO_3}$  and  $m$  are the amount of CaCO<sub>3</sub> nanoparticles and grafted silane coupling agent, respectively. The grafted amount of modifiers also can be easily calculated by the weight loss (between 200 °C and 670 °C) of modified nanoparticles minus the corresponding weight loss of unmodified ones. In equation (2),  $\eta$  is the theoretical grafting ratio equal to the amount of silane coupling agent used initially. According to the equations above, the weight loss behavior of varied samples is shown in Table 2. It can be seen that, with the increase of the amount of silane coupling agent, the grafting efficiency increased, while the utilization ratio dropped.

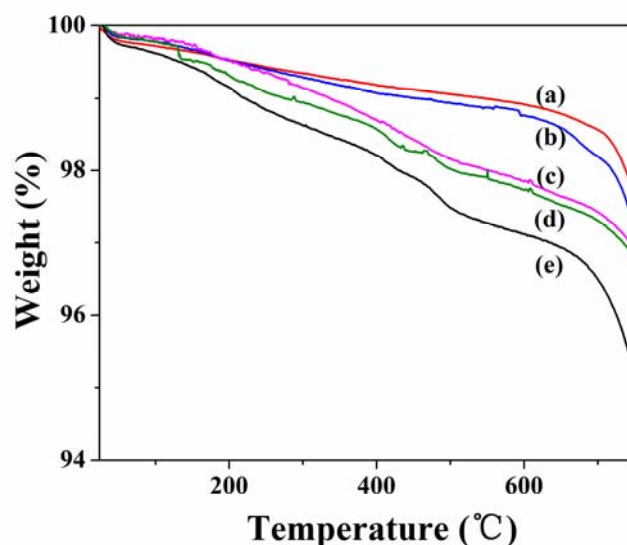


Fig. 2. TGA curves of  $\text{CaCO}_3$  nanoparticles modified with varied amounts of silane coupling agent (wt %): (a) 0, (b) 1, (c) 3, (d) 5 and (e) 7

Table 2. TGA-based weight losses of nanoparticles modified with varied amounts of silane coupling agent (from 200 °C to 670 °C)

Sample No.	silane coupling agent (wt %)	Weight loss (%)	Grafting ratio of silane coupling agent (%)	Utilization ratio of silane coupling agent (%)
(a)	0	0.8	0	—
(b)	1	1.1	0.3	30.0
(c)	3	1.9	1.1	36.7
(d)	5	2	1.2	24.0
(e)	7	2.3	1.5	21.4

### 3.3 XRD analysis

In order to investigate the effect of surface modification on the crystalline structure of  $\text{CaCO}_3$  nanoparticles, X-ray diffraction curves are presented in Fig. 3. Many strong X-ray diffraction peaks from  $20^\circ$  to  $50^\circ$  can be observed, and their corresponding Miller indices are marked out on the picture. The native  $\text{CaCO}_3$  nanoparticles used in the experiment is calcite based on the standard JCPDS (No. 85-1108). Apparently, the peaks are well-matched and no new peaks appear in curves (b), (c), (d) and (e), suggesting that surface modification did not alter the crystalline structure of  $\text{CaCO}_3$  nanoparticles. This behavior is similar to Zhang's research results [21]. However, an interesting phenomenon can be observed in Fig. 3 that diffraction peaks of modified  $\text{CaCO}_3$  nanoparticle sample shift to a small value regularly with the increasing amount of silane coupling agent, which is consistent with the previous report of Tang [22]. This variation can be explained by Bragg equation:

$$2d\sin\theta = n\lambda, n=1, 2, 3\dots \quad (3)$$

In equation (3),  $\lambda = 0.154$  nm,  $n = 1$  for remarkable strong diffraction peaks and  $d$  is the distance of crystal face. Therefore, the reduction of  $\theta$  value is due to the increase of the distance of crystal face after modification.

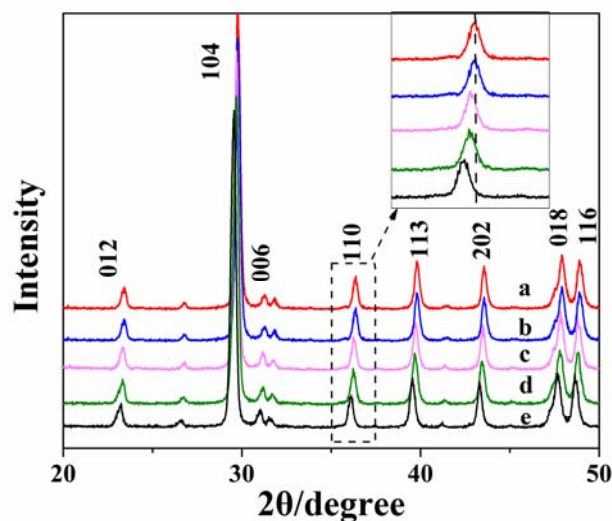
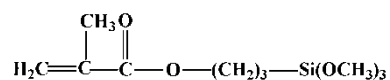


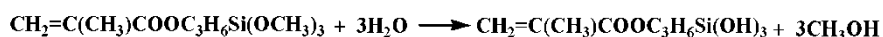
Fig. 3. XRD curves of  $\text{CaCO}_3$  nanoparticles modified with varied amounts of silane coupling agent (wt %): (a) 0, (b) 1, (c) 3, (d) 5 and (e) 7

### 3.4 Modification mechanism analysis

Silane coupling agent is widely used in surface modification of materials and it can be expressed by the formula:  $\text{RSiX}_3$ . R is usually some kinds of long carbon chains with hydrophobic groups and X stands for these groups which can easily hydrolyze. Chemical structural formula of silane coupling agent (KH570) is shown as below:



$\text{Si-OH}$  is formed after the alcoholysis reaction as presented in Fig. 4a, and then reacts with the hydroxyl groups on the surface of materials. According to the analysis of TGA, FTIR and XRD above, silane coupling agent was not physically adsorbed onto the surface of  $\text{CaCO}_3$  nanoparticles but formed a new chemical bond considered as  $\text{Ca-O-Si}$ . As shown in Fig. 4b,  $\text{RSi}(\text{OH})_3$  may form three  $\text{Ca-O-Si}$  chemical bonds, leading to surface exclusion and steric hindrance effects so that the surface free energy was reduced and the dispersion was improved after modification. It may be conducted as the reaction mechanism of the surface modification [11, 23].



a

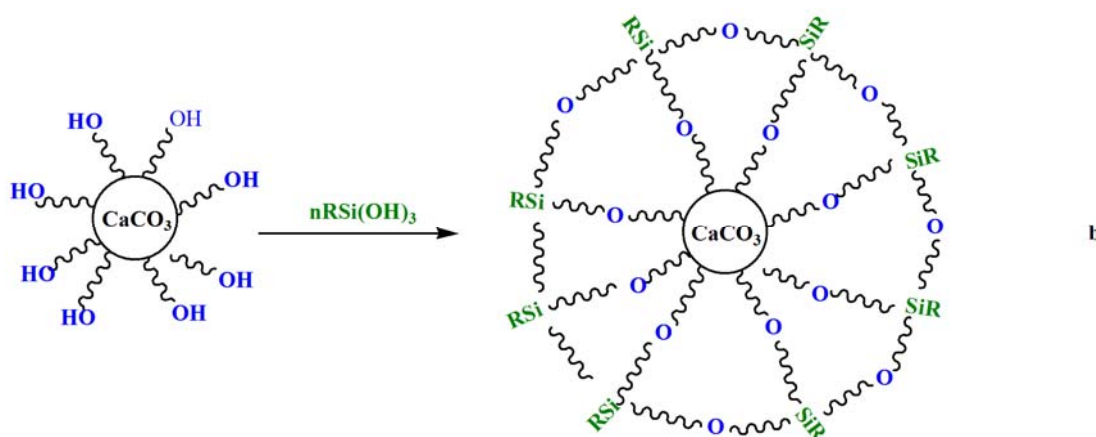


Fig. 4. Surface modification scheme of  $\text{CaCO}_3$  nanoparticles with silane coupling agent ( $R$  denotes  $\text{CH}_2=\text{C}(\text{CH}_3)\text{COOC}_3\text{H}_6$ )

### 3.5 Surface contact angle and surface free energy

Surface contact angle test was introduced to discuss the changes of surface properties of  $\text{CaCO}_3$  nanoparticles. The surface contact angle for water is presented in Fig. 5. After surface modification, surface contact angle value of  $\text{CaCO}_3$  nanoparticle sample increases from  $0^\circ$  to  $103.2^\circ$ , suggesting increased surface hydrophobicity property. The  $-\text{OH}$  on the surface of  $\text{CaCO}_3$  nanoparticles reacts with silane coupling agent which is hydrophobic because of the long carbon backbone ( $\text{CH}_2=\text{C}(\text{CH}_3)\text{COOC}_3\text{H}_6$ ). On one hand, this reaction may explain the changes described above, and on the other hand, the changes indicate that silane coupling agent is successfully grafted onto the surface of  $\text{CaCO}_3$  nanoparticles.

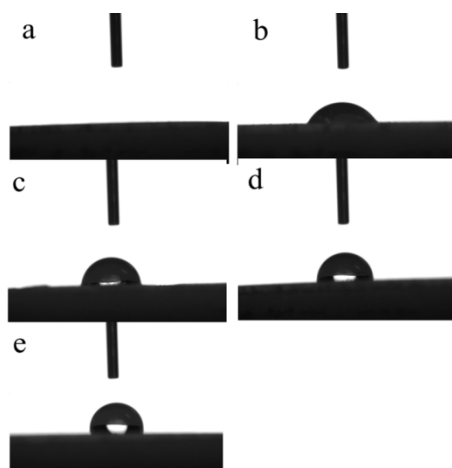


Fig. 5. Surface water contact angle of  $\text{CaCO}_3$  nanoparticles modified with different amounts of silane coupling agent (wt %): (a) 0, (b) 1, (c) 3, (d) 5 and (e) 7

To estimate the surface free energy of  $\text{CaCO}_3$  nanoparticles, the surface contact angle values for benzene were also measured. The surface free energy results were obtained with equations (4), (5) and (6) proposed by Owens [24]:

$$\gamma_L = \gamma_L^D + \gamma_L^P \quad (4)$$

$$\gamma_S = \gamma_S^D + \gamma_S^P \quad (5)$$

$$\gamma_L(1 + \cos \theta) = 2(\gamma_S^D \gamma_L^D)^{1/2} + 2(\gamma_S^P \gamma_L^P)^{1/2} \quad (6)$$

Where  $\gamma_L$  and  $\gamma_S$  are the surface energy of the liquid and the solid, respectively.  $\gamma_L^D$ ,  $\gamma_L^P$ ,  $\gamma_S^D$  and  $\gamma_S^P$  are the dispersion and the polar force components of the surface free energy of the liquid and the solid, respectively. The corresponding parameters of benzene and water are listed in Table 3. The polar force component of the surface free energy reflects the surface properties of materials, and small polar force surface free energy indicates good hydrophobic properties. Table 4 shows the results of surface free energy which was calculated based on Table 3 as well as equations (4), (5) and (6). As can be seen, with the increase of silane coupling agent used in the modification, the surface free energy of CaCO<sub>3</sub> nanoparticle samples and the polar force component decrease. While the dispersion force components of surface free energy increase slightly. When the amount of modifier is 7 wt %, the contact angle values for benzene and water are 19.6° and 103.2°, respectively. Compared with native CaCO<sub>3</sub> nanoparticles, the  $\gamma_S$  decreases 62.6% and  $\gamma_S^P$  drops from 58.23 mJ•m<sup>-2</sup> to 0.27 mJ•m<sup>-2</sup>. The high surface free energy of CaCO<sub>3</sub> nanoparticles is caused by the hydroxyl groups on the surface. After surface modification, the surface of CaCO<sub>3</sub> nanoparticles samples is covered with silane coupling agent, resulting in the decrease of surface free energy and its polar force component of nanoparticles. It suggests that the surface properties of CaCO<sub>3</sub> nanoparticles changed from absolutely hydrophilic to almost hydrophobic.

Table 3. The surface free energy of benzene and water ( $\gamma_L^D$  and  $\gamma_L^P$  are the dispersion and the polar force components of the surface free energy of the liquid, respectively).

Liquid	$\gamma_L^P$ (mJ•m <sup>-2</sup> )	$\gamma_L^D$ (mJ•m <sup>-2</sup> )	$\gamma_L$ (mJ•m <sup>-2</sup> )
benzene	0	28.9	28.9
water	51	21.8	72.8

Table 4. The contact angle values of CaCO<sub>3</sub> nanoparticle samples modified with varied amount of silane coupling agent and their corresponding surface free energy, the dispersion and the polar force components of the surface free energy

Silane coupling agent (wt %)	Contact angle(°)		$\gamma_S^P$ (mJ•m <sup>-2</sup> )	$\gamma_S^D$ (mJ•m <sup>-2</sup> )	$\gamma_S$ (mJ•m <sup>-2</sup> )
	benzene	water			
0	62.8	0	58.23	15.34	73.57
1	43.1	61.3	20.28	21.63	41.90
3	29.2	85.6	4.82	25.34	30.17
5	23.5	95.4	1.56	26.55	28.11
7	19.6	103.2	0.27	27.25	27.52

### 3.6 TEM observations

The TEM images of CaCO<sub>3</sub> nanoparticles before and after modification with 5 wt % silane coupling agent are shown in Fig. 6. It can be seen from Fig. 6a that the native commercial CaCO<sub>3</sub> nanoparticles are aggregated in aqueous solution with irregular shape, which is ascribed to its high surface energy and surface polarity. However, the dispersion of CaCO<sub>3</sub> nanoparticles gets notably improved after surface modification, as shown in Fig. 6b. This may be ascribed to the reduction of surface free energy and the increase of steric hindrance effects, which are caused by the macromolecular chains of silane coupling agent grafted onto the surface of nanoparticles.

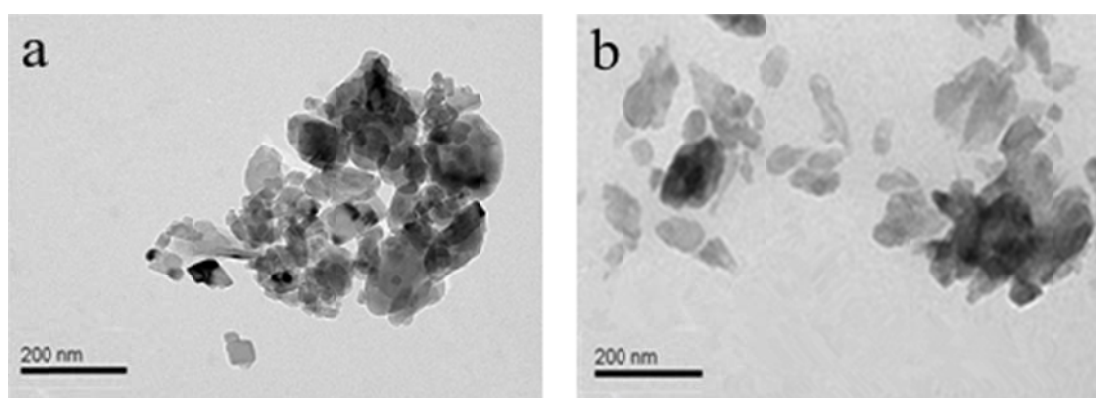


Fig. 6. Transmission electron microscope (TEM) images of CaCO<sub>3</sub> nanoparticles (a) unmodified and (b) modified with 5 wt % amount of silane coupling agent

### 3.7 Rheological properties of CaCO<sub>3</sub>/SBR nano-composites

CaCO<sub>3</sub> nanoparticles after surface modification were dispersed in SBR latex and CaCO<sub>3</sub>/SBR nano-composites were obtained. Rheological measurement of CaCO<sub>3</sub>/SBR nano-composites was exploited to evaluate the interfacial compatibility between CaCO<sub>3</sub> nanoparticles and SBR latex. Fig. 7(a) shows the steady shear stress curves attained for nano-composites containing CaCO<sub>3</sub> nanoparticles modified with varied amounts of silane coupling agent. In order to describe the rheological behavior of nano-composites accurately and completely, Herschel-Bulkley model was introduced to simulate their experimental data on the flow behavior of CaCO<sub>3</sub>/SBR nano-composites:

$$\tau = \tau_y + k\dot{\gamma}^n \quad (7)$$

Where  $\dot{\gamma}$  and  $\tau_y$  is the shear stress and yield stress respectively,  $k$  and  $n$  is the fluid consistency and fluid behavior index respectively, and  $\dot{\gamma}$  is the shear rate in fluid. Correspondingly, the rheological parameters of CaCO<sub>3</sub>/SBR nano-composites are listed in Table 5. In Table 5,  $n$  value indicates that all the CaCO<sub>3</sub>/SBR nano-composites display pseudoplastic behavior, exhibiting an evident decline in apparent viscosity with the increase of shear rate from 1 s<sup>-1</sup> to 500 s<sup>-1</sup>. In Fig. 7(b), for the nano-composites containing CaCO<sub>3</sub> nanoparticles modified with 3 wt % silane coupling agent, when the shear rate increases from 1 s<sup>-1</sup> to 500 s<sup>-1</sup>, the viscosity decreases from

0.14 Pa·s to 0.04 Pa·s. This decline trend is more apparent for the nano-composites containing CaCO<sub>3</sub> nanoparticles modified with a bigger amount of silane coupling agent. This can be assigned to the deformation and breakdown of the structured pigments and the flocs, which depends on the concentration of nano-composites. In addition, surface modification of CaCO<sub>3</sub> nanoparticles was found to play an important role in the viscosity behaviors of CaCO<sub>3</sub>/SBR nano-composites. As shown in Fig. 7(b), at the same shear rate, with the increase of silane coupling agent amount used to modify CaCO<sub>3</sub> nanoparticles, the viscosity of CaCO<sub>3</sub>/SBR nano-composites is on the visible decrease. The explanation for this is that surface modification can improve the hydrophobicity property and reduce the surface free energy of CaCO<sub>3</sub> nanoparticles, which is much closer to that of SBR latex.

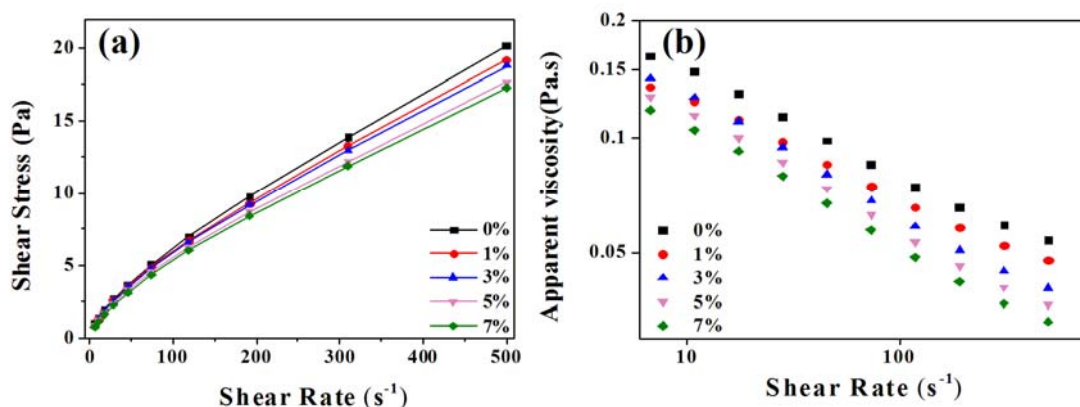


Fig. 7. Shear stress (a) and shear viscosity (b) as a function of the shear rate for the CaCO<sub>3</sub>/SBR nano-composites containing CaCO<sub>3</sub> nanoparticles modified with varied amounts of silane coupling agent

Table 5. Rheological parameters from Herschel-Buckley model of CaCO<sub>3</sub>/SBR nano-composites containing CaCO<sub>3</sub> nanoparticles modified with varied amounts of silane coupling agent

Silane coupling agent (wt %)	$\tau\gamma$ (Pa)	$k$ (Pa s <sup>n</sup> )	$n$	Standard error
0	0.1060	0.2041	0.7371	6.733
1	0.0464	0.2092	0.7254	6.605
3	0.0691	0.2060	0.7242	6.764
5	0.0352	0.2011	0.7185	7.202
7	0.0238	0.1856	0.7280	6.318

#### 4. Conclusions

The surface of CaCO<sub>3</sub> nanoparticles was modified with silane coupling agent, which was designed to improve the nanoparticle dispersion and interfacial compatibility between CaCO<sub>3</sub> nanoparticles and styrene-butadiene rubber (SBR) latex. The results revealed that silane coupling agent was successfully grafted onto the surface of CaCO<sub>3</sub> nanoparticles. When the utilization

efficiency and grafting ratio of silane coupling agent were taken into consideration, 5 wt% was a suitable amount. After surface modification, the nanoparticle dispersion and hydrophobicity of CaCO<sub>3</sub> nanoparticles were improved distinctly. Through rheological measurement, at the same shear rate, with the increasing amount of silane coupling agent used to modify CaCO<sub>3</sub> nanoparticles, the viscosity of CaCO<sub>3</sub>/SBR nano-composites decreases obviously, indicating that surface modification can greatly improve the interfacial compatibility of CaCO<sub>3</sub> nanoparticles with styrene-butadiene rubber (SBR) latex.

### Acknowledgment

The research is grateful for the financial support from the National Natural Science Foundation of China (Grant No. 31100442), Open Foundation of State Key Laboratory of Pulp and Paper Engineering of China (Grant No. 200818).

### References

- [1] H. Du, S.W. Lee, J. Gong, C. Sun, L.S. Wen. *Mater. Lett.* **58**, 1117 (2004)
- [2] D.G. Peng, J.S. Zhang, Q.L. Liu, E.W. Taylor. *J. Inorg. Biochem.* **101**, 1457 (2007)
- [3] A. Hoffman, A. Lafosse, Sh. Michaelson, M. Bertin, R. Azria. *Surf. Sci.* **602**, 3026 (2008)
- [4] J. Vigié, J. Sukmanowski, B. Nölting, F. Royer. *Colloids Surf. A* **302**, 269 (2007)
- [5] S. Suzuki. *Colloids Surf. A* **202**, 81-91 (2002)
- [6] M. Fujiwara, K. Shiokawa, K. Morigaki, Y.C. Zhu, Y. Nakahara. *Chem. Eng. J.* **137**, 14 (2008)
- [7] C.X. Gu, Q.Z. Li, Z.M. Gu, G.Y. Zhu. *J. Rare Earths* **26**, 163 (2008)
- [8] M.J. Cai, J.D. Chen. *Mod. Plast. Process. Appl.* **21**, 1 (2009)
- [9] D. Shan, Y.N. Wang, H.G. Xue, S. Cosnier. *Sens. Actuators B* **136**, 510 (2009)
- [10] X.Q. Wang, D.G. Jiang. *J. China Univ. Min. Technol.* **18**, 76 (2008)
- [11] C. Xue, Y.C. Zhu, B. Zhou, Y.P. Guo, W. Gao, Y.J. Ma, S. Guan, L.W. Wang, Z.C. Wang. *Powder Technol.* **204**, 21-26 (2010)
- [12] F. Morel, V. Bounor-Legaré, E. Espuche, O. Persyn, M. Lacroix. *Eur. Polym. J.* **48**, 919-929 (2012)
- [13] H.V. Tran, L.D. Tran, H.D. Vu, H. Thai. *Colloids Surf. A* **366**, 95 (2010)
- [14] Y.J. Tang, Y.M. Li, J. Song, Z.D. Pan. *Acta Phys. -Chim. Sin.* **23**, 717 (2007)
- [15] M. Sabzi, S.M. Mirabedini, J. Zohuriaan-Mehr, M. Atai. *Prog. Org. Coat.* **65**, 222 (2009)
- [16] J. Zhao, M. Milanova, M.M.C.G. Warmoeskerken, V. Dutschk. *Colloids Surf. A* (in press)
- [17] D.L. Jin, L.H. Yue, Z.D. Xu. *Chinese J. Inorg. Chem.* **20**, 715 (2004)
- [18] E. Ukaji, T. Furusawa, M. Sato, N. Suzuki. *Appl. Surf. Sci.* **254**, 563 (2007)
- [19] X.X. Li, B.Y. Zheng, L.M. Xu, D.D. Wu, Z.L. Liu, H.C. Zhang. *Rare Metal Mat. Eng.* **41**, 24 (2012)
- [20] J.Q. Zhang, H.X. Feng, X. Zhao, H.M. Luo, D. Zhao. *Chem. Reag.* **31**, 5 (2009)
- [21] L. Zhang, M. Zhong, H.L. Ge. *Appl. Surf. Sci.* **258**, 1551 (2011)
- [22] Y.J. Tang, Y.M. Li, J. Song, Z.D. Pan. *Chinese J. Inorg. Chem.* **22**, 2018 (2006)
- [23] M.Y. Lou, D.P. Wang, W.H. Huang, D. Chen, B. Liu. *J. Magn. Mater.* **305**, 83 (2006)
- [24] D. K. Owens, R. C. Wendt. *J. Appl. Polym. Sci.* **13**, 1741 (1969)